

Ultrastructure of fenestrations in endothelial choriocapillaries of the rabbit—a freeze-fracturing study

S. MELAMED,¹ I. BEN-SIRA,¹ AND Y. BEN-SHAUL²

From the ¹Department of Ophthalmology, Beilinson Medical Center, Tel-Aviv University, Petah-Tikva, Israel, and the ²Department of Microbiology, George S. Wise Faculty of Life Sciences, Tel-Aviv University, Tel-Aviv, Israel

SUMMARY Replicas of freeze-fractured endothelial cells of normal rabbits' choriocapillaries were studied. Differences in fenestral appearance on the E face and P face could be detected. E face pores appeared as circular craters containing particulate material arranged at the pores' rim and a central diaphragm. Mean pore diameter was 78.5 nm, average diaphragm size 30 nm, and peripheral particle size 12.3 nm. In several pores possible radiating connections between diaphragm and peripheral particles could be observed. Pores in the P face appeared as vallate papillae, with a circular, particulate, elevated rim surrounding a shallow surface and a central accumulation of particles resembling the diaphragm. The diameter of P face pores was found to be 76.5 nm, with a diaphragm size of 23.7 nm, and peripheral particle size of 12.7 nm. The calculated space between peripheral particles and diaphragm was 12.0 nm for the E face and 12.7 nm for the P face. With the Markham method a regular pattern of 8 peripheral particles at the pores' rim was observed on both E face and P face. A possible 3-dimensional model of the choriocapillary endothelial fenestration is presented. This model consists of 8 peripheral particles which are connected with a central diaphragm creating a space of 12.0–12.7 nm between them. This sieve-like structure and the calculated passage size fit well with the 'small pore' theory of molecular permeability.

A knowledge of the structural and physiological aspects of the choroidal endothelial fenestration is essential for understanding macromolecular permeability to the external retina. In the choriocapillary endothelium transmission electron microscopy studies have shown a diaphragm in the centre of the pore in cross and tangential sections.¹⁻⁴ This finding was reconfirmed by other investigators using the freeze-fracture technique.^{5,6} More thorough ultrastructural studies of the pores were carried out on fenestrae in other organs, such as kidney, pancreas, and intestinal tract.⁷⁻¹⁰ Maul,¹⁰ studying the rat kidney, suggested an octagonal shape for the pores' rim, and assumed that the central diaphragm consists of 2 rings. Clementi and Palade¹¹ showed that peroxidase molecules, about 5nm in size, could pass more freely through the intestinal fenestrae than ferritin molecules, 11 nm in size.

Bill¹² showed that uveal capillaries are more permeable to myoglobin (4 nm) than to albumin (7 nm) and to albumin more than to gammaglobulin (11 nm). The aim of this study was to determine whether the intrafenestral ultrastructure can be correlated with the special permeability properties of the choriocapillaries.

Materials and methods

Four albino rabbits of 2.5–3.0 kg body weight were anaesthetised with 30 mg/kg pentobarbitone sodium injected intravenously. After deep anaesthesia was achieved one eye of each rabbit (4 eyes) was enucleated; other eyes were used for another study. The enucleated globes were cut in 0.1 M cacodylate buffer. The retina was gently stripped from the choroid, and then the choroid was carefully removed from the sclera. The choroidal tissue was immediately immersed in a solution of 2.5% glutaraldehyde in 0.1 M cacodylate buffer and fixed at 4°C overnight. After fixation the samples of tissue were

Correspondence to Dr S. Melamed, Beilinson Medical Center, Department of Ophthalmology, Petah-Tikva, Israel.

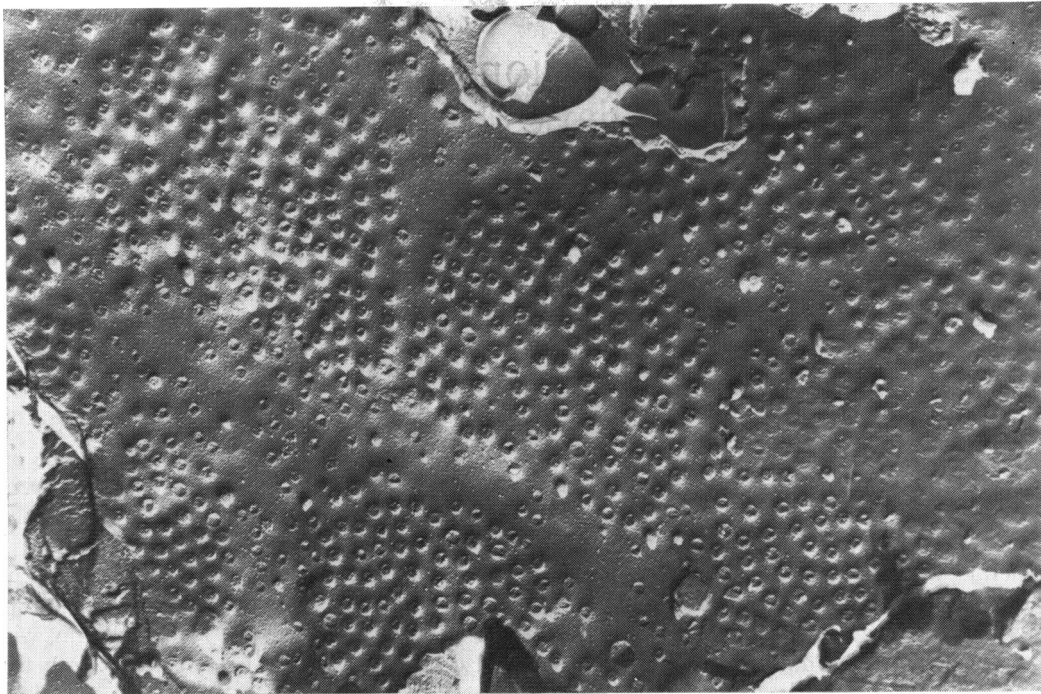


Fig. 1 Freeze-fractured replica of endothelial cell membrane showing groups of fenestrations separated by smooth cytoplasmic areas. ($\times 24\ 000$).

washed several times with cacodylate buffer and suspended overnight in 30% glycerol in the same buffer at 4°C. Samples 2–3 mm in size were frozen in Freon 22, transferred immediately to liquid nitrogen, and freeze-fractured in a Balzer's freeze-etching unit, according to the standard procedures.¹³ All preparations were examined and photographed in a Jeol-100B electron microscope at 80 kb.

Results

In the replicas of freeze-fractured tissue the choriocapillaries were easily identified because of their proximity to Bruch's membrane and the characteristic appearance of the fenestrae. In surface view of the endothelial cell groups of closely packed fenestrations were separated by nonfenestrated, relatively smooth cytoplasmic areas. Most of the fenestrae observed were circular; some which were cleaved obliquely had an oval rather than circular shape (Fig. 1).

At higher magnifications the differences between fenestrae exposed in different split membranes were more evident. On the E face¹⁴ the pores appeared as circular craters containing particulate material arranged at the pores' rim and a central

diaphragm. The diaphragm appeared either as a smooth face or as a cluster of small particles, the appearance presumably depending on the cleavage plane. The peripheral particles seemed to be regularly arranged close to the rim in many fenestrae, especially in those cleaved tangentially. Structures which looked like radiating rays could be observed in some pores, connecting the peripheral particles with the central diaphragm (Fig. 2). On the P face the fenestrae appeared as vallate papillae. They seemed to be protruded, with a circular raised, particulate rim surrounding a shallower surface. In the crater a cluster of particles resembling the diaphragm could frequently be observed (Fig. 3).

A histogram of 120 pores has been drawn recording the fenestral diameter, peripheral particle size, and diameter of the diaphragm. Measurement of the diaphragm diameter presented some difficulty because of the inconsistency in appearance of the diaphragms due to differences in the cleavage plane. Consequently the measurements were either of the smooth central area or of the diameter of clustered particles. Of the 120 pores measured 48 were on the E face and 72 on the P face. Only circular, regular, tangentially cleaved pores were selected for measurement. Measurements of the fenestrae and

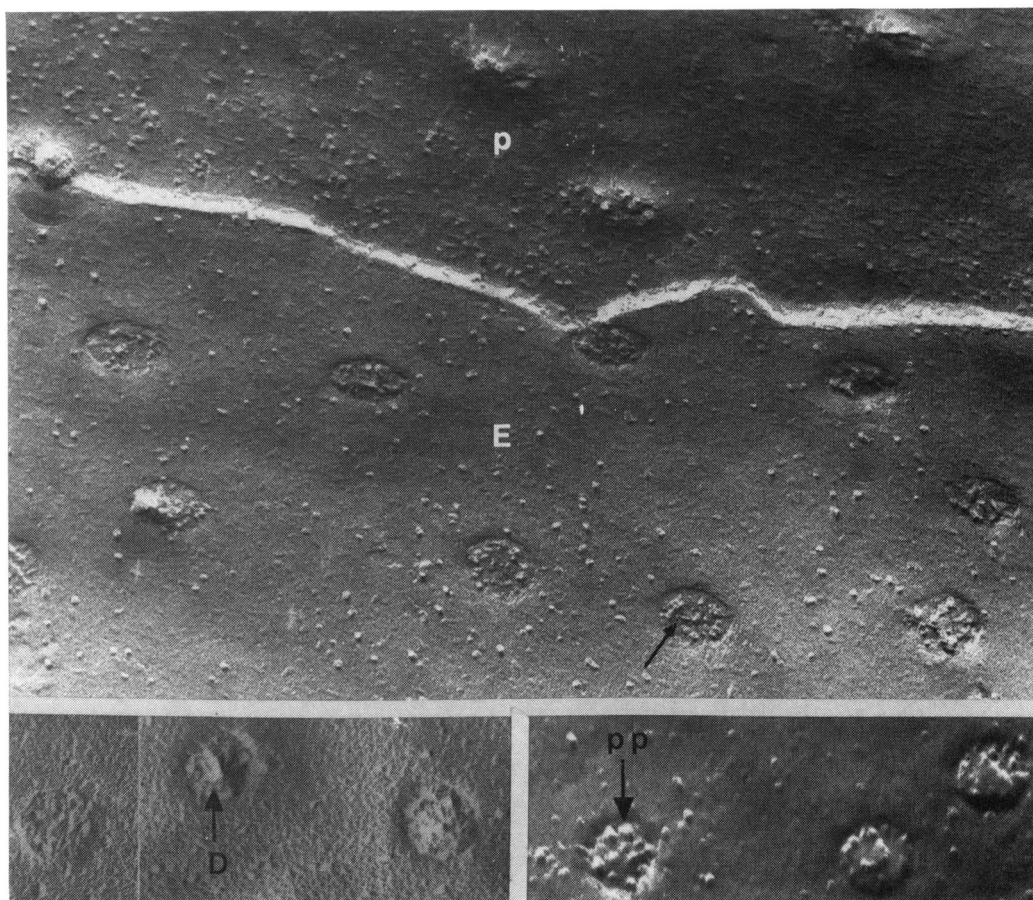


Fig. 2 Replica showing both E face (E) and P face (P) of a cleaved endothelial cell membrane. The arrow indicates possible connections between diaphragm and peripheral particles. Peripheral particles (pp) and diaphragm (D) shown below. ($\times 132\,000$).

their substructures on both fractured faces are shown (Fig. 4). For uniformity prints were enlarged to give $1\text{ mm} = 9.6\text{ nm}$. The calculated average diameter of the pores on the E face is 78.5 nm . That of the central diaphragm is 30 nm , and the size of each peripheral particle is approximately 12 nm . Thus the calculated average space between the peripheral particle and the diaphragm is about 12 nm . On the P face the average diameter of the fenestration was found to be 76.5 nm , of the diaphragm 23.7 nm , and of the peripheral particles 13.8 nm , thus leaving a space of 12.7 nm . Details are summarised in Table 1.

By means of the Markham technique,¹⁵ pores were rotated on a printing stage. Ten circular, tangentially cleaved fenestrae on the E face and seven on the P face were selected and printed in a different number of rotations ($n=3, 4, 5, 7, 8$, and

Table 1 Average size of pores and their subunits on E and P face

	Size in nm	
	E face	P face
Pore diameter	78.5	76.5
Diaphragm diameter	30.0	23.7
Size of a peripheral particle	12.3	13.8
Calculated space between diaphragm and peripheral particles	12.0	12.7

10). Enhancement of peripheral particles was maintained in all pores when they were rotated 8 times. It is therefore assumed that there is a regular structural pattern of 8 particles at the pore's rim on both E face and P face (Fig. 5).

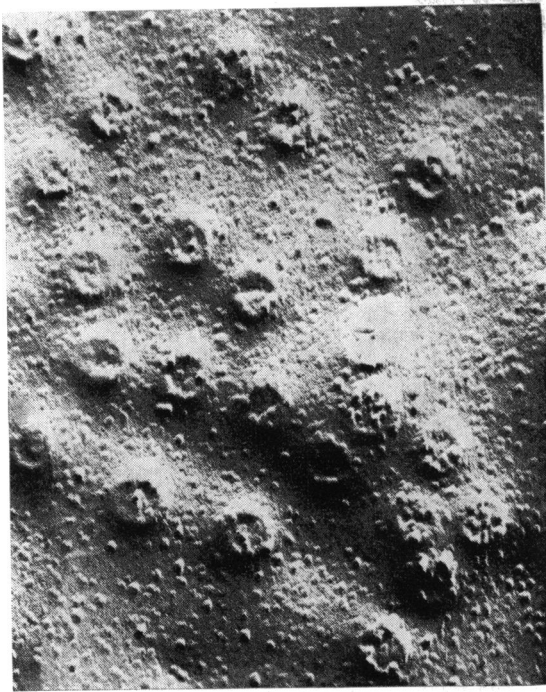


Fig. 3 P face of a cleaved endothelial cell membrane. Note the elevated particulate rim and central clusters of particles representing the diaphragm. ($\times 87\,570$).

Discussion

The ultrastructure of capillary fenestrae in the kidney, pancreas, and intestinal tract has already been described in some detail.⁷⁻¹⁰ In the choriocapillaries the existence of a diaphragm or central density was confirmed by thin sectioning and freeze-fracturing.¹⁻⁶ Spitznas *et al.*⁵ have described the diaphragm as a central thickening measuring approximately 30 nm, while fenestral diameter in their material was found to be 60 nm. Raviola⁶ has also described a central diaphragm in freeze-fractured replicas of choriocapillary fenestrations, but no measurements were carried out. Hogan *et al.*,³ describing thin sections of pores, found their diameter to be about 80 nm. Our study confirms the random distribution of fenestrae interrupted by cytoplasmic areas as described in the mouse renal papilla,⁷ and for the human choriocapillaries.⁵ In addition our finding of mean pore diameter is closer to that found by Hogan *et al.*³ We found the pore diameter to be 78.5 nm on the E face and 76.5 nm on the P face. The central diaphragm diameter was found to be about 30 nm on the E face (similar to the reported size of 30 nm by Spitznas *et al.*⁵) and 23.7 nm on the P face. The

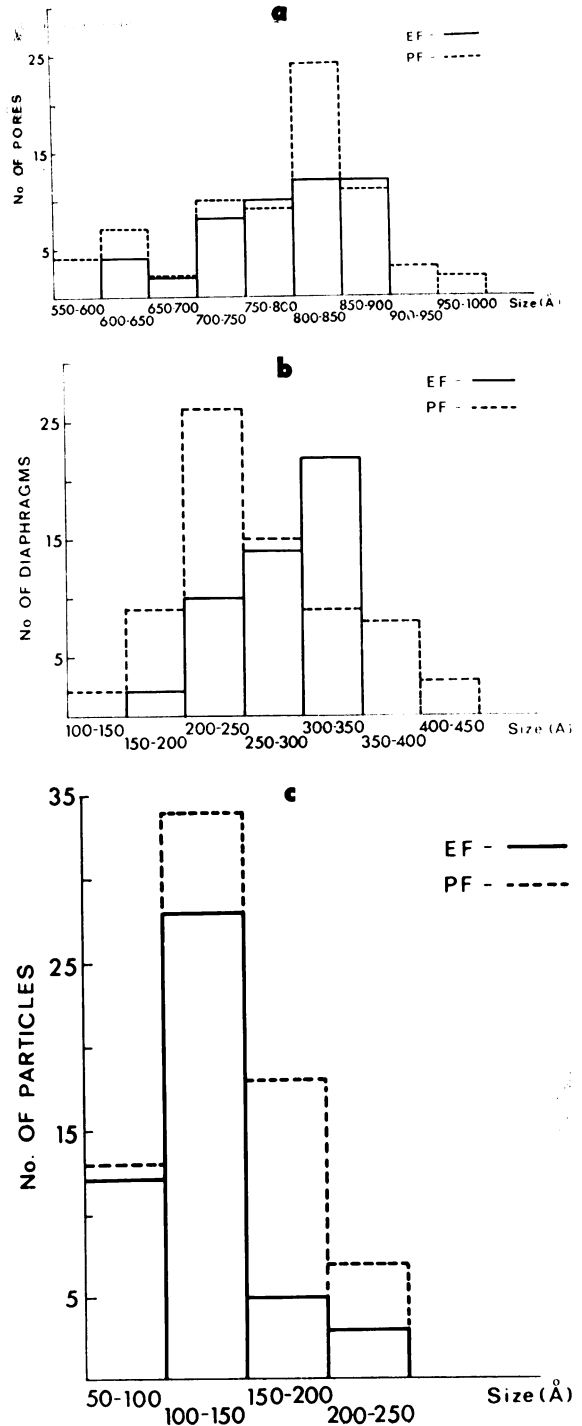


Fig. 4 Histograms showing size distributions of fenestral elements. a. Pore's diameter. b. Diameter of diaphragm, c. Size of peripheral particles.

difference between diaphragm measurement on the E face and P face is attributed mainly to difficulties in measurements, as stated above.

In our study we have postulated the existence of peripheral particles at the pore's rim. Eight regularly arranged particles were shown and their

octagonal pattern was enhanced repeatedly by the Markham method¹⁵ in different pores, implying a consistent substructure. In occasional pores fine radiating rays could be observed connecting the peripheral particles with the diaphragm. The existence of such connections raises the possibility that

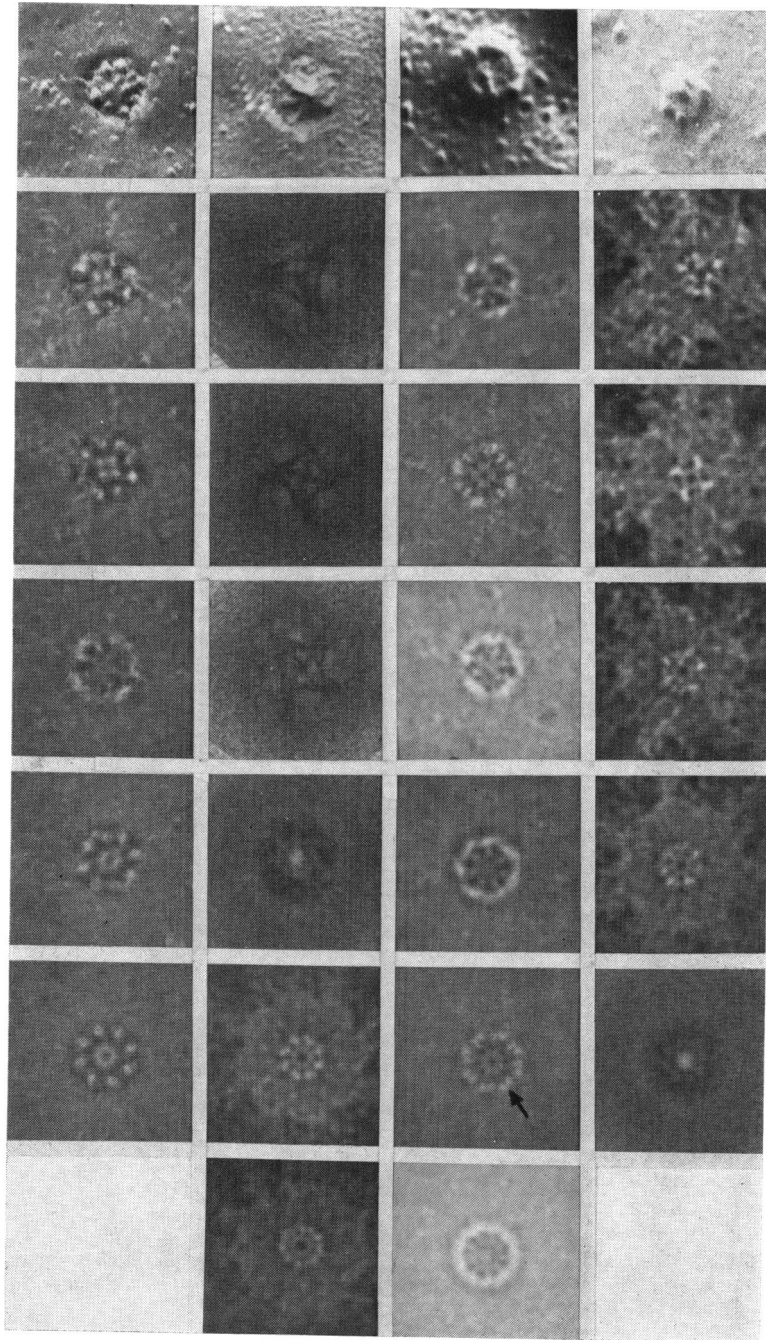


Fig. 5 Rotation of pores according to the Markham method. Top row shows the unrotated prints. The 2 on the left side are pores on the E face, the 2 on the right are on the P face. Rows 2, 3, 4, 5, 6, 7 represent rotations of $n=3, 4, 5, 7, 8,$ and 10 respectively. Marked enhancement results at $n=8$ rotations. Note (arrow) that occasionally enhanced P face particles looked as if composed of 2 subunits.

Fig. 6 Schematic drawing of possible cleavage planes within the fenestrae. A. Cleavage plane splitting the Bruch's membrane orientated side. B. Cleavage plane splitting the scleral orientated side. C. Cleavage plane passing by the fenestral elements.

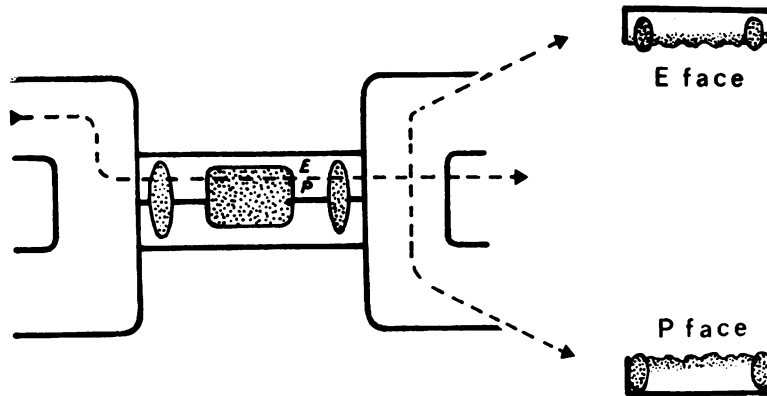


Fig. 7 Schematic presentation of possible integral proteins crossing the fused membranes which form the fenestration. Possible cleavage planes through these integral proteins are also depicted.

these intrafenestral structures may be involved in the control of macromolecular leakage by active stretching and relaxing of the diaphragm, thus changing the diameter of the passages available for macromolecular permeability from the choroid to the retina. This study was not aimed at investigating the occurrence of contractile elements associated with the peripheral particles. The possibility that the intrafenestral system acts as a sieve-like mechanism cannot be excluded and deserves a further study.

The calculated space of 12.0–12.7 nm between diaphragm and peripheral particles corresponds well with the 'small pore' theory, enabling small molecules such as peroxidase (5 nm) to pass through the pores, while larger molecules like ferritin (11 nm) cannot pass freely.¹¹ If, as suggested by Maul,¹⁰ the pore is created by fusion of the 2 adjacent membranes, one has to presume that the appearance of the fenestrae on the P face would fit with its counterpart on the E face. This is true to a limited extent. The pattern of practically all pores on the P face, when compared to each other, was found to be similar; the same applies to those observed on the E face. However, it would be expected that if the peripheral particles on one face are protruding, the other fractured face will show their imprints, namely, small shallow 'craters'. That was not the case, as protruding peripheral particles were observed on both fractured faces. A possible

explanation might be that the protruding particles observed on both faces represent 2 halves or 2 subunits of integral proteins which cross the 2 fused membranes, and that the cleavage plane passed through them rather than around them.

The possible cleavage planes within the fenestral elements are schematically depicted (Fig. 6). A possible cleavage plane sparing the diaphragm (above it or below it), thus creating a smooth face inside the pore, is also included. Several pores of that appearance were encountered. If the pore elements are considered to be formed as a result of

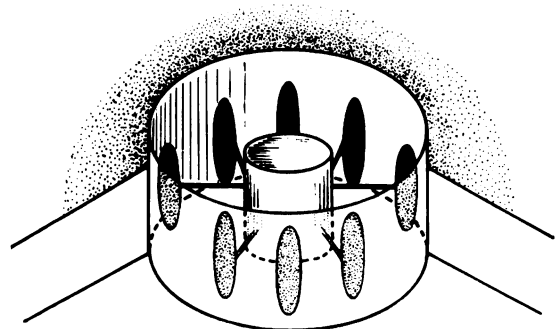


Fig. 8 A possible 3-dimensional model of a chorio-capillary endothelial fenestration. The calculated space between diaphragm and peripheral particles was found to be 12.0–12.7 nm.

adhesion or fusion of endothelial cell membranes, the P faces should be adjacent to the centre of the pore, while the E faces are external. The similarity of practically all E face pores and P face pores favours the possibility of a symmetrical arrangement at the width of the pores' element.

Fig. 7 shows schematically why the repeatedly protruding particles on both the E face and P face might be explained by the passage of the cleavage plane through the postulated integral proteins. Having described the regularity of the 8 peripheral particles with their average size and possible connections with the diaphragm, we suggest a possible 3-dimensional model of the fenestration in the choriocapillary (Fig. 8).

This study was supported by a grant from the Israeli Ministry of Health.

References

- ¹Garron LK. The ultrastructure of the retinal pigment epithelium, with observations on the choriocapillaries and Bruch's membrane. *Trans Am Ophthalmol Soc* 1970; **61**: 545-76.
- ²Matsusaka T. Ultrastructural differences between the choriocapillaries and retinal capillaries on the human eye. *Jpn J Ophthalmol* 1970; **14**: 59-67.
- ³Hogan MJ, Alvarado JA, Weddell JE. *Histology of the Human Eye. An Atlas and Textbook*. Philadelphia: Sanders, 1971: 370.
- ⁴Spitznas M. The fine structure of the chorioretinal border tissues of the adult human eye. *Adv Ophthalmol* 1974; **28**: 78-86.
- ⁵Spitznas M, Reale E. Fracture faces of fenestrations and junctions of endothelial cells in human choroidal vessels. *Invest Ophthalmol* 1975; **14**: 98-107.
- ⁶Raviola G. The structural basis of the blood-ocular barriers. *Exp Eye Res (Suppl.)* 1977; 27-63.
- ⁷Friederici HHR. The tridimensional ultrastructure of fenestral capillaries. *J Ultrastruct Res* 1962; **6**: 171-92.
- ⁸Friederici HHR. On the diaphragm across fenestrae of capillary endothelium. *J Ultrastruct Res* 1969; **27**: 373-5.
- ⁹Simionescu M, Simionescu N, Palade GE. Morphometric data on the endothelium of blood capillaries. *J Cell Biol* 1974; **60**: 128-52.
- ¹⁰Maul GG. Structure and formation of pores in fenestrated capillaries. *J Ultrastruct Res* 1971; **36**: 768-82.
- ¹¹Clementi F, Palade GE. Intestinal capillaries—permeability to peroxidase and ferritin. *J Cell Biol* 1969; **41**: 33-58.
- ¹²Bill A. Capillary permeability to and extravascular dynamics of myoglobin, albumin and gammaglobulin in the urea. *Acta Physiol Scand* 1968; **73**: 204-19.
- ¹³Moor H, Mühlethaler K. Fine structure in frozen-etched yeast cells. *J Cell Biol* 1963; **17**: 609-28.
- ¹⁴Branton D, Bullivant S, Gilula JB, et al. Freeze etching nomenclature. *Science* 1975; **190**: 54-6.
- ¹⁵Markham R, Frey S, Hills BJ. Methods of enhancement of image detail and accentuation of structure in electron microscopy. *Virology* 1963; **20**: 88-102.